Innovative method for simultaneous electrical and thermal parametrisation of automotive batteries

Thomas R. B. Grandjean, Andrew McGordon, Widanalage D. Widanage
Energy and Electrical Systems, WMG
University of Warwick
Coventry, CV4 7AL. UK
T.Grandjean@Warwick.ac.uk

***Abstract*—Coupled electro-thermal models are essential for the battery management system (BMS) to accurately predict the electrical and temperature dynamics of automotive batteries. Currently, an electrochemical model and a thermal model are developed and parametrised separately before being coupled together. A new procedure known as pulse-multisine (PM) has been developed that combines a multisine and a pulse signal, which allows for concurrent electrochemical and thermal parametrisation from the same experiements. A non-linear Equivalent Circuit Model and an analogous lumped parameter thermal model are parametrised and validated against automotive drive cycles. Despite the procedure requiring fewer experiments, the model has increased accuracy.**

Keywords*—simultaneous parametrisation, battery management system, battery thermal maganagement system, pulse multisine, equivalent circuit model, lumped parameter thermal model

I. INTRODUCTION

With ever increasing endorsement of legislation to reduce carbon emissions, such as the EU 2020 targets [1], and rapidly escalating concerns over local air pollution [2], the automotive industry is actively developing alternative technologies to reduce its dependence on fossil fuels [3]. Lithium ion batteries have become the prevailing choice for modern environmentally friendly vehicles due to their relatively high energy and power densities, long cycle life, lack of memory effect, and low self-discharge rates [4].

Due to the wide operating voltage, lithium ion batteries require organic electrolytes, which are highly flammable and volatile [5]. In addition to safety concerns, the temperature sensitivity of the conductivity of the organic electrolyte makes lithium ion battery properties, such as internal resistance and capacity, more temperature dependent than other types of batteries [6]. Experiments performed at different ambient temperatures have revealed that the ageing rate has a strong temperature dependence, often described by the Arrhenius equation [7–10]. Operating cells at elevated temperatures (>25˚C) is known to accelerate SEI film growth on the anode and degradation of the cathode, leading to capacity fade and increased internal impedance [10], the latter producing more heat and accelerating ageing further in a positive feedback loop. It is therefore critical for the battery management system (BMS) to accurately predict the electrical and hence temperature dynamics of the battery.

Coupled electro-thermal models vary in complexity. The electrical characteristics may be described by simple equivalent circuit models (ECM) [11–16] or PDE based models [17–20], whilst the thermal aspects can be captured by simple two state models [21–23] or complex thermal models that describe the temperature distribution of the cell [24–26]. Although the more complex models are highly accurate, they are difficult to parametrise and require large computational capabilities, rendering them unsuitable for control oriented applications such as BMS modelling. The electro-thermal model therefore needs to couple an electrical ECM with an analogical thermal model.

Electro-thermal models available in the literature are characterised from separate experiments [13, 23, 27]. First the ECM parameters are estimated from two experiments: an Open Circuit Voltage (OCV) test followed by either Electrochemical Impedance Spectroscopy (EIS) or Hybrid Pulse Power Characterisation (HPPC) methods. The second part is to estimate the thermal parameters from a separate third experiment.

A new procedure known as pulse-multisine (PM) has been developed [28] that combines a multisine and a pulse signal, which allows for concurrent electrochemical and thermal parametrisation. This reduces the number of experiments required to develop the model.

II. METHODOLOGY

A. Pulse multisine

Multisine excitations are commonly employed in system identification to measure the frequency response of a nonlinear system and have not been applied to lithium ion batteries until recently [29]. Instead of dividing the overpotential at a fixed time point by the magnitude of the current pulse to obtain the internal resistance of the cell, an equivalent circuit model (ECM) is fitted to a more dynamic (in amplitude and frequency) response. ECMs are a relatively simple lumped parameter model ubiquitous in estimation algorithms for describing lithium ion batteries electrochemical behaviour in real time [30–33]. Whilst this does increase the measurement calculation complexity, it improves the model accuracy [28]. Performing a least squares fit to the whole voltage response is also more robust than a simple division of two measurements.

Furthermore the battery is excited with a more dynamic current signal, both in terms of amplitude and frequency, compared to the HPPC technique [28, 34]. This PM signal is a periodic signal that is generated by summing sinusoids, providing the researcher with the flexibility to alter the amplitude spectrum and harmonic content. In terms of the frequency spectrum, the signal provides a better representative estimate data set than a DC pulse, i.e. during operation automotive battery drive cycle demands are not simple square pulses but continuous signals containing a range of frequencies. In addition to improving model accuracy over the desired frequency spectrum, this characterisation approach covers a wide current range during a short excitation current signal, allowing a broad and more representative current range to be characterised.

The PM signal allows for concurrent thermal characterization as it heats up the lithium ion battery by circa 1-2˚C. The lumped parameter thermal model is fitted to the measured surface temperature during the PM signal.

B. Models

The coupled electro-thermal model is comprised of two sub models: a non-linear ECM (NL-ECM) and a lumped parameter thermal model.

1) NL-ECM

The NL-ECM consists of three components, i.e. a linear ECM, a nonlinear over-voltage function $f(v_l)$ and an OCV coupled with hysteresis as shown in Fig. 1.

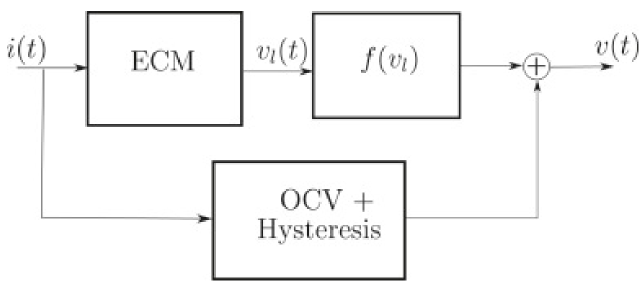

Fig. 1. Non linear equivalent circuit model

The linear ECM is a second-order RC network model commonly used to decribed the terminal voltage of lithium ion batteries [35]. The nonlinear over-voltage function accounts for the Tafel relation in electrochemical kinetics, where a higher over-potential is required to sustain a given current density at low SoCs and temperatures [28]. The third component characterises the OCV and hysteresis as per the method proposed in [36].

2) Lumped parametmer thermal model

The thermal model is a first order thermal model as shown in Fig. 2, where q is the heat generation rate [Js^{-1}], θ_1 is the surface temperature [K], R is the thermal resistance [KW^{-1}], C is the heat capacity [JK^{-1}], and θ_A is the ambient temperature.

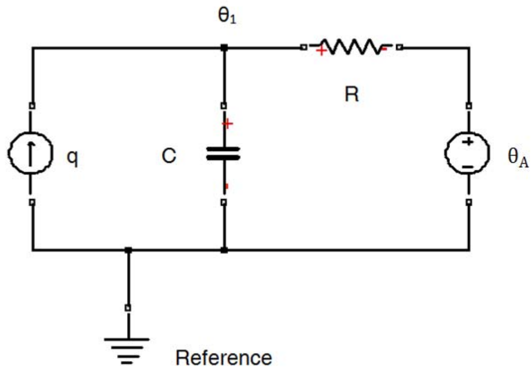

Fig. 2. Lumped parameter thermal model

The heat generation q in the cell is governed by the polarisation heat from joule heating and energy dissipated in the electrode potential [24], given by

$$q = \eta I \tag{1}$$

Where η is the overpotential (the difference between the OCV and the battery terminal voltage) calculated by the NL-ECM and I is the input current. The effect of entropic heat generation is not included since it has been shown to be negligible at high C-rates for NCA batteries [37].

C. Structural Identifiability

Given a model circuit diagram, it is possible to describe mathematically the exact relationship between the input and the output of the model. As this relationship depends on the model structure (i.e., the circuit diagram), it is simply referred to as the input/output structure. Usually, there are unknown model parameters in this relationship that need to be estimated from empirical data. Given an input/output structure and some proposed experiments to collect data for parameter estimation, structural identifiability analysis considers the uniqueness of the unknown model parameters. It is a purely theoretical method that assumes the data is perfect and noise-free [38, 39]. This is an important, but often overlooked, theoretical prerequisite to experiment design, system identification, and parameter estimation, since numerical estimates for unidentifiable parameters are effectively meaningless; unidentifiable parameters have an infinite number of possible numerical solutions. If parameter estimates are to be used to inform about charging and discharging strategies, or other critical decisions, then it is essential that the parameters be uniquely identifiable. Parameter-fitting software packages generally struggle when attempting to estimate nonidentifiable parameters; numerical optimisation algorithms may oscillate between numerous possible solutions, considerably reducing the confidence in the accuracy of the parameter values.

Numerous techniques for performing a structural identifiability analysis on linear parametric models exist, and this is a well-understood topic [38–40]. The Laplace transform approach, or transfer function approach, is normally the method selected to analyse linear models; see [41] for a thorough discussion of this method.

1) NL-ECM

The NL-ECM utilised is nonlinear due to hysteresis and the nonlinear overvoltage function. The Laplace transform approach is not applicable to nonlinear systems. The structural identifiability of a simple second-order RC network with hysteresis has been established previously [42]. The nonlinear overvoltage function is also structurally identifiable since it is a sigmoid fit of measured vs modelled over-voltage.

2) Lumped parametmer thermal model

The first order thermal model can be described by the following input/output relationship:

$$\frac{d\theta_1}{dt} = \frac{qR + \theta_A - \theta_1}{RC} \tag{2}$$

Given $\boldsymbol{p}$ is the r dimensional vector of unknown parameters [R, C], a second input/output map is generated by substituting $\boldsymbol{p}$ for $\tilde{\boldsymbol{p}}$ in the original map, Equating the monomials of these two functions produces only one solution for the unknown parameters therefore the system is structurally globally identifiable.

Similar analysis of a second order thermal model yields the following input/output relationship:

$$\frac{d^2\theta_2}{dt^2} = \frac{qR_2 + \theta_A - \theta_2 - \left(R_1C_1 + R_2C_1 + R_2C_2\right)\frac{d\theta_2}{dt}}{R_1C_1R_2C_2} \tag{3}$$

Which is structurally unidentifiable from surface temperature measurements alone. Additional information, such as internal temperature, is required to parametrise the second order model uniquely.

D. Experiments

In this work the current to voltage relationship of five 18650 3.03Ah $LiNiCoAlO_2$ (NCA) batteries are modelled using pulse-multisine current signals. Model parameters are obtained over different SoCs and temperatures, a pulse-multisine is applied at five SoCs which were, 10%, 20%, 50% 80% and 95% and at four temperatures 0 °C, 10 °C, 25 °C and 45 °C to parametrise the model. The surface temperature of each cell was measured using a K-type thermocouple.

III. Results

A. Parametrisation

The parameters for the NL-ECM have been published previously [28] and are not repeated for brevity. The global thermal parameters fitted simultaneously over five cells at five SoCs (10%, 20%, 50% 80% and 95%), and at four temperatures (0 °C, 10 °C, 25 °C and 45 °C) are shown in TABLE I. . Although in total 100 datasets were collected, the global thermal parameters were only fitted against 94 datasets since some datasets had to be discarded due to experimental issues such as thermocouples detaching from the cell surface.

TABLE I. shows that the maximum error (fitted temperature vs measured temperature) is within the K-type thermocouple measurement accuracy of ±1.5°C.

TABLE I. Fitted thermal parameters

Parameter	Value
Resistance	$R = 6.23\ KW^{-1}$
Conductance	$K^T = 0.160\ WK^{-1}$
Capacitance	$C = 83.4\ JK^{-1}$
Root Mean Square Deviation	0.19°C
Maximum error	1.39°C

Fig. 3 displays a sample of ten datasets from the simultaneous fit and confirms excellent visual goodness of fit. All 94 datasets are not displayed for brevity.

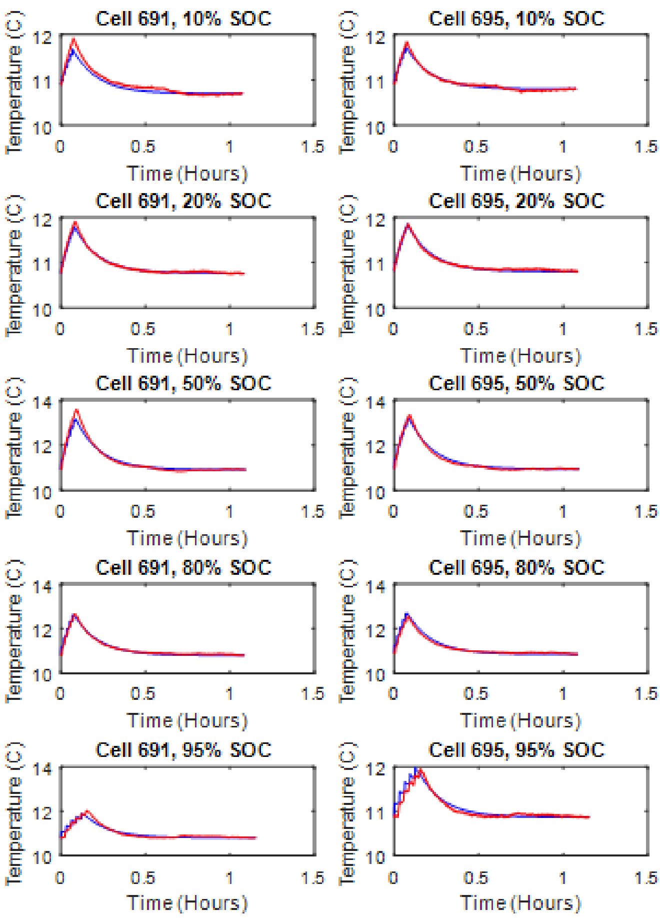

Fig. 3. Sample of simultaneous thermal model

B. Validation

The coupled electro-thermal model is validated with the US Environmental Protection Agency (EPA) Urban Dynamometer Driving Schedule (UDDS) [43] at 0˚C ambient temperature. The 1369 seconds signal is looped from 75% SoC until the cell is discharged to 0% SoC. The validation results are presented in Fig. 4.

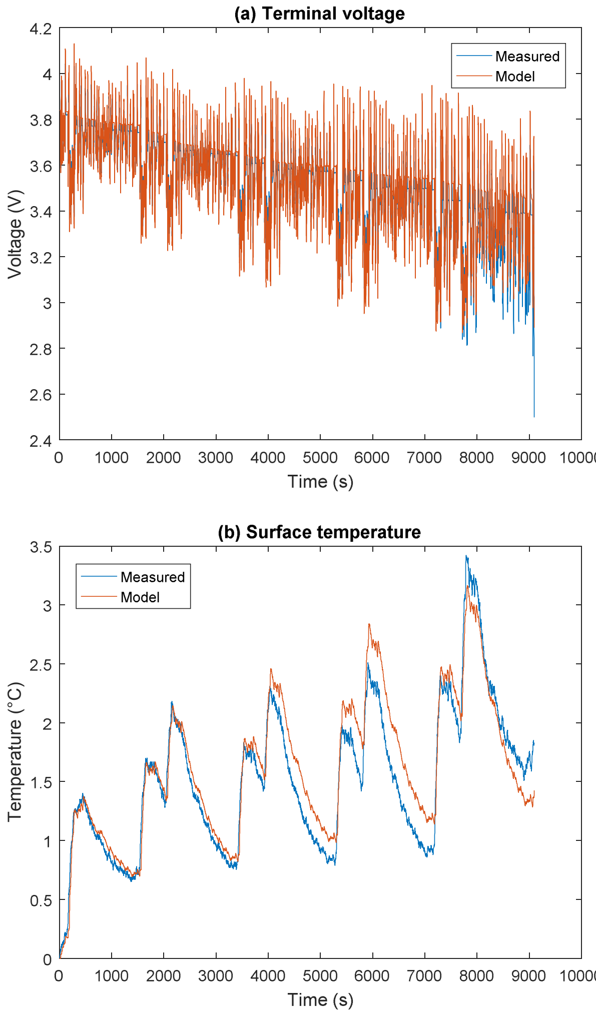

Fig. 4. UDDS Validation drive cycle at 0˚C ambient temperature

Fig. 4(a) shows the measured battery terminal voltage and the model prediction. The Root Mean Square Deviation (RMSD) is 52.9mV compared with 60.2mV for the PM method without the thermal feedback (12% improvement).

Fig. 4(b) shows the measured battery surface temperature and the model predicted. The RMSD is 0.2˚C.

IV. Discussion

The NL-ECM characterised with PM has previously been shown to have lower root mean square deviation and peak error when compared to a linear ECM estimated using pulse data [28]. Coupling the NL-ECM with a first order lumped parameter thermal model further improves the lower root mean square deviation and peak error for automotive drive cycles. Furthermore, the proposed model predicts cell surface temperature, which can be used by the BMS to monitor and reduce ageing effects and maintain the lithium ion cells efficiently within their safe operation window. Accurately predicting surface temperature also reduces the requirement to instrument each cell with thermal sensors in electric vehicle battery packs.

The main advantage of this coupled electo-thermal model is that no further experiments are required since the thermal parameters are estimated from the same experiments required to parametrise the electrochemical model. In addition, the proposed coupled electro-thermal model is very fast to simulate and can be operated in real time within electric vehicle BMS, whilst providing improved accuracy to current models available in the literature.

A. Further work

Additional experiments are being performed on instrumented cells in order to couple the NL-ECM with a second order lumped parameter thermal model that is able to predict both the surface and the core temperature.

V. Conclusion

The coupled electro-thermal model proposed yields a 12% lower root mean square deviation and peak error when compared to a NL-ECM without thermal feedback and does not require any further experiments to estimate the thermal parameters since the PM method to characterise the NL-ECM is also used to parametrise the thermal sub model.

Aknowledgment

The research presented within this paper is supported by the Innovate UK (https://hvm.catapult.org.uk/) through the WMG centre High Value Manufacturing (HVM) Catapult in collaboration with Jaguar Land Rover and TATA Motors.

References

[1] The European Parliament and the Council of the European Union, ‘Regulation (EU) No 333/2014 of the European Parliament and of the Council of 11 March 2014 Amending Regulation (EC) No 443/2009 to Define the Modalities for Reaching the 2020 Target to Reduce CO2 Emissions From New Passenger Cars’, *Off. J. Eur. Union*, vol. L103, pp. 15–21, 2014.

[2] J. H. Seinfeld and S. N. Pandis, *Atmospheric chemistry and physics : from air pollution to climate change*. Hoboken, NJ, USA: John Wiley & Sons, 2016.

[3] K. G. Høyer, ‘The history of alternative fuels in transportation: The case of electric and hybrid cars’, *Util. Policy*, vol. 16, no. 2, pp. 63–71, 2008.

[4] K. E. Aifantis, S. A. Hackney, R. V. Kumar, and Wiley InterScience (Online service), *High energy density lithium batteries : materials, engineering, applications*. Hoboken, NJ, USA: John Wiley & Sons, 2010, 2010.

[5] Q. Wang, P. Ping, X. Zhao, G. Chu, J. Sun, and C. Chen, ‘Thermal runaway caused fire and explosion of lithium ion battery’, *J. Power Sources*, vol. 208, pp. 210–224, 2012.

[6] S. Al Hallaj, H. Maleki, J. S. Hong, and J. R. Selman, ‘Thermal modeling and design considerations of lithium-ion batteries’, *J. Power Sources*, vol. 83, no. 1, pp. 1–8, 1999.

[7] B. Y. Liaw, E. P. Roth, R. G. Jungst, G. Nagasubramanian, H. L. Case, and D. H. Doughty, ‘Correlation of Arrhenius behaviors in power and capacity fades with cell impedance and heat generation in cylindrical lithium-ion cells’, *J. Power Sources*, vol. 119, pp. 874–886, 2003.

[8] S. Käbitz *et al.*, ‘Cycle and calendar life study of a graphite|LiNi1/3Mn1/3Co1/3O2 Li-ion high energy system. Part A: Full cell characterization’, *J. Power Sources*, vol. 239, pp. 572–583, 2013.

[9] M. Ecker *et al.*, ‘Calendar and cycle life study of Li(NiMnCo)O2-based 18650 lithium-ion batteries’, *J. Power Sources*, vol. 248, pp. 839–851, 2014.

[10] T. Waldmann, M. Wilka, M. Kasper, M. Fleischhammer, and M. Wohlfahrt-Mehrens, ‘Temperature dependent ageing mechanisms in Lithium-ion batteries – A Post-Mortem study’, *J. Power Sources*, vol. 262, pp. 129–135, 2014.

[11] K. Smith, G.-H. Kim, E. Darcy, and A. Pesaran, ‘Thermal/electrical modeling for abuse-tolerant design of lithium ion modules’, *Int. J. Energy Res.*, vol. 34, no. 2, pp. 204–215, Feb. 2010.

[12] Lijun Gao, Shengyi Liu, and R. A. Dougal, ‘Dynamic lithium-ion battery model for system simulation’, *IEEE Trans. Components Packag. Technol.*, vol. 25, no. 3, pp. 495–505, Sep. 2002.

[13] R. Benger, H. Wenzl, H.-P. Beck, M. Jiang, D. Ohms, and G. Schaedlich, ‘Electrochemical and thermal modelling of lithium ion cells for use in HEV or EV application’, *World Electr. Veh. J.*, vol. 3, pp. 342–351, 2009.

[14] T. Huria, M. Ceraolo, J. Gazzarri, and R. Jackey, ‘High fidelity electrical model with thermal dependence for characterization and simulation of high power lithium battery cells’, in *2012 IEEE International Electric Vehicle Conference*, 2012, pp. 1–8.

[15] V. Sangwan, A. Sharma, R. Kumar, and A. K. Rathore, ‘Estimation of battery parameters of the equivalent circuit models using meta-heuristic techniques’, in *2016 IEEE 1st International Conference on Power Electronics, Intelligent Control and Energy Systems (ICPEICES)*, 2016, pp. 1–6.

[16] Y. Li, D. M. Vilathgamuwa, T. W. Farrell, San Shing Choi, and N. T. Tran, ‘An equivalent circuit model of li-ion battery based on electrochemical principles used in grid-connected energy storage applications’, in *2017 IEEE 3rd International Future Energy Electronics Conference and ECCE Asia (IFEEC 2017 - ECCE Asia)*, 2017, pp. 959–964.

[17] W. B. Gu and C. Y. Wang, ‘Thermal-Electrochemical Modeling of Battery Systems’, *J. Electrochem. Soc.*, vol. 147, no. 8, p. 2910, 2000.

[18] W. Fang, O. J. Kwon, and C.-Y. Wang, ‘Electrochemical-thermal modeling of automotive Li-ion batteries and experimental validation using a three-electrode cell’, *Int. J. Energy Res.*, vol. 34, no. 2, pp. 107–115, Feb. 2010.

[19] C. Y. Wang and V. Srinivasan, ‘Computational battery dynamics (CBD)—electrochemical/thermal coupled modeling and multi-scale modeling’, *J. Power Sources*, vol. 110, no. 2, pp. 364–376, Aug. 2002.

[20] P. Kemper and D. Kum, ‘Extended Single Particle Model of Li-Ion Batteries Towards High Current Applications’, in *2013 IEEE Vehicle Power and Propulsion Conference (VPPC)*, 2013, pp. 1–6.

[21] C. Park and A. K. Jaura, ‘Dynamic Thermal Model of Li- Ion Battery for Predictive Behavior in Hybrid and Fuel Cell Vehicles.’, in *2003 Future Transportation Technology Conference : SAE technical paper*, 2003.

[22] X. Lin *et al.*, ‘Parameterization and Observability Analysis of Scalable Battery Clusters for Onboard Thermal Management’, *Oil Gas Sci. Technol. — Rev. IFP Energies Nouv.*

[23] C. Forgez, D. Vinh Do, G. Friedrich, M. Morcrette, and C. Delacourt, ‘Thermal modeling of a cylindrical LiFePO4/graphite lithium-ion battery’, *J. Power Sources*, vol. 195, no. 9, pp. 2961–2968, 2010.

[24] D. Bernardi, E. Pawlikowski, and J. Newman, ‘A General Energy Balance for Battery Systems’, *J. Electrochem. Soc.*, vol. 132, no. 1, p. 5, 1985.

[25] A. Samba *et al.*, ‘Development of an Advanced Two-Dimensional Thermal Model for Large size Lithium-ion Pouch Cells’, *Electrochim. Acta*, vol. 117, pp. 246–254, Jan. 2014.

[26] U. Iraola, I. Aizpuru, J. M. Canales, A. Etxeberria, and I. Gil, ‘Methodology for thermal modelling of lithium-ion batteries’, in *IECON 2013 - 39th Annual Conference of the IEEE Industrial Electronics Society*, 2013, pp. 6752–6757.

[27] H. E. Perez, J. B. Siegel, X. Lin, A. G. Stefanopoulou, Y. Ding, and M. P. Castanier, ‘Parameterization and Validation of an Integrated Electro-Thermal Cylindrical LFP Battery Model’, in *Volume 3: Renewable Energy Systems; Robotics; Robust Control; Single Track Vehicle Dynamics and Control; Stochastic Models, Control and Algorithms in Robotics; Structure Dynamics and Smart Structures;*, 2012, pp. 41–50.

[28] W. D. Widanage *et al.*, ‘Design and use of multisine signals for Li-ion battery equivalent circuit modelling. Part 1: Signal design’, *J. Power Sources*, vol. 324, pp. 70–78, 2016.

[29] D. A. Howey, P. D. Mitcheson, V. Yufit, G. J. Offer, and N. P. Brandon, ‘Online Measurement of Battery Impedance Using Motor Controller Excitation’, *IEEE Trans. Veh. Technol.*, vol. 63, no. 6, pp. 2557–2566, Jul. 2014.

[30] H. He, R. Xiong, and J. Fan, ‘Evaluation of Lithium-Ion Battery Equivalent Circuit Models for State of Charge Estimation by an Experimental Approach’, *Energies*, vol. 4, no. 12, pp. 582–598, Mar. 2011.

[31] D. Chen, J. Jiang, X. Li, Z. Wang, and W. Zhang, ‘Modeling of a Pouch Lithium Ion Battery Using a Distributed Parameter Equivalent Circuit for Internal Non-Uniformity Analysis’, *Energies*, vol. 9, no. 11, p. 865, Oct. 2016.

[32] A. Nikolian *et al.*, ‘Lithium Ion Batteries—Development of Advanced Electrical Equivalent Circuit Models for Nickel Manganese Cobalt Lithium-Ion’, *Energies*, vol. 9, no. 5, p. 360, May 2016.

[33] K. Uddin, A. Picarelli, C. Lyness, N. Taylor, and J. Marco, ‘An Acausal Li-Ion Battery Pack Model for Automotive Applications’, *Energies*,

vol. 7, no. 9, pp. 5675–5700, Aug. 2014.

[34] W. D. Widanage *et al.*, 'Design and use of multisine signals for Li-ion battery equivalent circuit modelling. Part 2: Model estimation', *J. Power Sources*, vol. 324, pp. 61–69, 2016.

[35] M. Dubarry and B. Y. Liaw, 'Development of a universal modeling tool for rechargeable lithium batteries', *J. Power Sources*, vol. 174, no. 2, pp. 856–860, Dec. 2007.

[36] A. Barai, W. D. Widanage, J. Marco, A. McGordon, and P. Jennings, 'A study of the open circuit voltage characterization technique and hysteresis assessment of lithium-ion cells', *J. Power Sources*, vol. 295, pp. 99–107, Nov. 2015.

[37] A. Eddahech, O. Briat, and J.-M. Vinassa, 'Thermal characterization of a high-power lithium-ion battery: Potentiometric and calorimetric measurement of entropy changes', *Energy*, vol. 61, pp. 432–439, 2013.

[38] R. Bellman and K. J. Åström, 'On structural identifiability', *Math. Biosci.*, vol. 7, no. 3, pp. 329–339, 1970.

[39] K. Godfrey and J. DiStefano, *Identifiability of model parameters*. Oxford: Pergamon, 1987.

[40] E. Walter, *Identifiability of parametric models*. Oxford: Pergamon Press, 1987.

[41] John A. Jacquez, *Compartmental Analysis in Biology and Medicine*. Ann Arbor, MI: BioMedware, 1996.

[42] T. Grandjean, A. McGordon, and P. Jennings, 'Structural Identifiability of Equivalent Circuit Models for Li-Ion Batteries', *Energies*, vol. 10, no. 1, p. 90, Jan. 2017.

[43] US EPA, 'EPA Urban Dynamometer Driving Schedule (UDDS)'. [Online]. Available: https://www.epa.gov/emission-standards-reference-guide/epa-urban-dynamometer-driving-schedule-udds. [Accessed: 30-Mar-2017].